

# Serial Changes in $^{14}\text{C}$ -Deoxyglucose and $^{201}\text{Tl}$ Uptake in Autoimmune Myocarditis in Rats

Naoki Tokita, Shinji Hasegawa, Eiichiro Tsujimura, Kenji Yutani, Tohru Izumi, and Tsunehiko Nishimura

Division of Tracer Kinetics, Biomedical Research Center, Osaka University Graduate School of Medicine, Osaka; and Department of Internal Medicine, Kitasato University School of Medicine, Sagamihara, Japan

This study was designed to examine the relationships between the uptake of  $^{14}\text{C}$ -deoxyglucose (DG) and the uptake of  $^{201}\text{Tl}$  in a rat model of autoimmune myocarditis. **Methods:** Autoimmune myocarditis was induced in normal rats by immunization with pig cardiac myosin. Dual-tracer autoradiography with DG and  $^{201}\text{Tl}$  was performed on frozen slices of the animals' hearts 3 wk (acute phase), 8 wk (subacute phase), and 14 wk (chronic phase) (each  $n = 5$ ) after immunization. The extent of inflammatory damage was classified histologically into three categories on the basis of cell infiltration: mild (Mi), moderate (Mo), and severe (Sv). The regional count in the region of interest set on the autoradiogram was normalized on the basis of that of control rats. The ratio of total cardiac uptake to the injected dose ( $\%ID/g \times BW$ , where ID is injected dose and BW is body weight) was calculated by tissue counting. Expressions of glucose transporters GLUT1 and 4 were evaluated by the enzyme-labeled antibody method. **Results:** The total cardiac uptake of DG in the acute phase of myocarditis was significantly higher than in normal control rats ( $3.43\% \pm 0.92\%$  vs.  $0.97\% \pm 0.38\%$ ;  $P < 0.0001$ ); it then decreased in the chronic phase but was still higher than in the controls ( $1.85\% \pm 0.37\%$  vs.  $0.97\% \pm 0.38\%$ ;  $P < 0.01$ ). The total cardiac uptake of  $^{201}\text{Tl}$  in the acute phase of myocarditis was significantly lower than in the controls ( $7.4\% \pm 0.7\%$  vs.  $12.0\% \pm 3.3\%$ ;  $P < 0.005$ ); it then increased in the chronic phase and reached normal levels ( $13.0\% \pm 3.3\%$  vs.  $12.0\% \pm 3.3\%$ ; not significant [NS]). In the acute phase, the regional uptakes of DG in the Mi, Mo, and Sv regions were  $143.1\% \pm 107.9\%$ ,  $169.6\% \pm 59.9\%$ , and  $317.5\% \pm 103.3\%$ , respectively, whereas those of  $^{201}\text{Tl}$  were  $88.4\% \pm 31.9\%$ ,  $72.1\% \pm 34.6\%$ , and  $48.4\% \pm 21.5\%$ , respectively. GLUT expression was evaluated visually and classified into four grades (0, 1, 2, and 3). In the acute phase, GLUT1 expression was higher in rats in the Sv group than in the controls (2.87 vs. 0.87). GLUT4 was not expressed in the Sv areas but was found in the Mi areas. **Conclusion:** In the acute phase of autoimmune myocarditis in rats, cardiac uptake of DG was accelerated by severe inflammation. Cardiac uptake of  $^{201}\text{Tl}$ , on the other hand, was suppressed. Our results suggest that GLUT1 expression accelerates DG uptake by cells in areas of severe inflammation.

**Key Words:** autoimmune myocarditis;  $^{14}\text{C}$ -deoxyglucose;  $^{201}\text{Tl}$ ; glucose transporter; autoradiography

**J Nucl Med 2001; 42:285–291**

**T**he prognosis of myocarditis patients depends greatly on both a diagnosis in the early stage and the initial treatment. The clinical symptoms and signs are often nonspecific, and conventional examinations for myocarditis, such as electrocardiograms, serum cardiac enzymes, and chest radiographs, are insensitive (1). The most specific changes in the heart that characterize myocarditis are the presence of numerous infiltrating cells and the appearance of giant cells (2). However, histologic methods require invasive procedures that carry a risk of accidental injury, making noninvasive diagnostic methods important for patients with myocarditis. Previous reports on myocarditis have included diagnostic studies with  $^{99m}\text{Tc}$ -pyrophosphate (3),  $^{67}\text{Ga}$ -citrate (4,5),  $^{131}\text{I}$ -antimyosin monoclonal antibody (5), and  $^{111}\text{In}$ -antimyosin Fab (4,6); FDG PET also detects inflammation (7,8). It has been proposed that FDG PET is more sensitive than other methods in detecting inflammation in the diagnosis of myocarditis.

This study assessed changes in glucose metabolism based on myocardial damage in the acute, subacute, and chronic phases of autoimmune myocarditis in rats by performing dual-tracer autoradiography with  $^{14}\text{C}$ -deoxyglucose (DG) and  $^{201}\text{Tl}$  on the hearts of affected animals.

## MATERIALS AND METHODS

### Induction of Autoimmune Myocarditis in Rats

Experimental myocarditis was induced in rats by immunizing them with cardiac myosin, as described previously (9). Cardiac myosin was purified from the porcine ventricular myocardium and was used as the antigen. It was dissolved to a concentration of 20 mg/mL in phosphate-buffered saline containing 0.3 mol/L KCl; then it was mixed with an equal volume of complete Freund's adjuvant containing 11 mg/mL *Mycobacterium tuberculosis* (Difco Laboratories, Detroit, MI). The antigen-adjuvant emulsion (0.2 mL) was injected subcutaneously into the footpads of Lewis rats (8-wk-old males; Charles River Japan, Inc., Yokohama, Japan). Control rats received 0.1 mL saline mixed with an equal volume of complete Freund's adjuvant. Rats were maintained under specific pathogen-free conditions in facilities for comparative medicine and animal experimentation at the Osaka University Graduate School of Medicine.

Received Mar. 15, 2000; revision accepted Aug. 14, 2000.  
For correspondence or reprints contact: Tsunehiko Nishimura, MD, PhD, Division of Tracer Kinetics, Biomedical Research Center, Osaka University Graduate School of Medicine, (D9) 2-2 Yamada-oka, Suita, Osaka 565-0871, Japan.

### Biodistribution Study of $^{201}\text{Tl}$ and DG

All rats fasted for more than 12 h before the studies. Three weeks (acute phase), 8 wk (subacute phase), and 14 wk (chronic phase) after immunization, rats were anesthetized with 1.0% isoflurane using a small animal anesthetizer (model TK-4; Bio Machinery, Funabashi, Japan). DG (370 kBq; Dupont NEN, Boston, MA) was injected through the tail vein, and  $^{201}\text{Tl}$  (18.5 MBq; Nihon Mediphysics, Nishinomiya, Japan) was injected 30 min later.  $^{201}\text{Tl}$  activity was measured with a  $\gamma$  scintillation counter (Curiementor 2; PTW-FREIBURG, Freiburg, Germany). Rats were killed by injection of saturated KCl 10 min after the  $^{201}\text{Tl}$  injection. The heart was excised, placed on filter paper, and weighed. The basal half of the heart was cut into small samples, and these samples were carefully weighed.

Myocardial uptake of  $^{201}\text{Tl}$  was measured with a  $\gamma$  counter (Auto-Gamma 5000; Packard, Meriden, CT) and calculated as follows:

$$\text{myocardial uptake (\%ID/g} \times \text{BW)} = \frac{\text{(myocardial radioactivity/HW)}}{\text{(totalID/BW)}}$$

where ID is injected dose, BW is body weight, and HW is heart weight.

One month after the rats were killed, which was sufficient time for  $^{201}\text{Tl}$  to decay, the sample was dissolved in 2 mL tissue solubilizer (Soluene-350; Packard, Downers Grove, IL). On complete dissolution, 12 mL liquid scintillator fluid (Hionic-fluor; Packard) were added to the sample, and  $\beta$  radioactivity was measured with a liquid scintillation counter (model 1414; Wallac Oy, Turku, Finland). Myocardial uptake of DG was calculated with the same equation used for  $^{201}\text{Tl}$  uptake above.

### Dual-Tracer Autoradiography

The same heart groups used in the biodistribution study were also prepared for autoradiography. Dual-tracer autoradiography with  $^{201}\text{Tl}$  and DG was performed in the acute, subacute, and chronic phases. Rats were initially injected intravenously with 370 kBq DG and then with 18.5 MBq  $^{201}\text{Tl}$  30 min later. Ten minutes after the  $^{201}\text{Tl}$  injection, the rats were killed by injection of saturated KCl. The heart was rapidly excised, rinsed with saline, and

incised in the midline. The apical side of the heart was rapidly embedded in Tissue Mount (Chiba Medical, Soka, Japan) and frozen in *n*-hexane cooled with dry ice. The frozen tissue was cut into 20- $\mu\text{m}$ -thick sections perpendicular to the short axis of both ventricles with a cryostat at  $-20^\circ\text{C}$ . The sections were mounted on a clean glass slide and quickly air-dried. To visualize  $^{201}\text{Tl}$ , the specimens were exposed to an imaging plate (BAS-SR 2025; Fuji Photo Film Co., Ltd., Tokyo, Japan) for 30 min. One month after the rats were killed, which was sufficient time for  $^{201}\text{Tl}$  to decay, the same section was exposed to an imaging plate for 3 d to visualize DG. Microscales of DG (Nycomed Amersham, Buckinghamshire, U.K.) were used to quantitate the regional DG uptake, and the image data were analyzed with a computerized imaging analysis system (BAS 5000 Mac; Fuji). Regions of interest (ROIs) (0.08  $\text{mm}^2$ ) were set on each autoradiogram, and the average count of all ROIs was calculated to quantitate the regional uptakes of  $^{201}\text{Tl}$  and DG.

### Histopathologic Assessment

Consecutive 5- $\mu\text{m}$ -thick myocardial tissue slices were cut and stained with hematoxylin and eosin. The extent of inflammatory cell infiltration and myocyte necrosis was evaluated by two independent observers.

The specimens were classified, according to the histologic degree of infiltration as follows: mild (a few infiltrating cells in a section), moderate (numerous infiltrating cells in a section but with the area of infiltration not exceeding 0.20  $\text{mm}^2$ ), and severe (numerous infiltrating cells in a section with the area of infiltration exceeding 0.20  $\text{mm}^2$ ) (Fig. 1).

### Immunohistochemistry

The 5- $\mu\text{m}$  sections were stained with polyclonal anti-GLUT1 and anti-GLUT4 antibodies (rabbit anti-GLUT1 AB 1340, anti-GLUT4 AB 1346; Chemicon International, Inc., Temecula, CA). The sections were incubated with anti-GLUT1 and anti-GLUT4 antibodies after preincubation with  $\text{H}_2\text{O}_2$  and goat albumin and then incubated with biotinylated antirabbit immunoglobulin (IgG) (second antibody; Vector Laboratories, Burlingame, CA). Finally, the bound antibody was visualized with horseradish peroxidase streptavidin (Vector). Consecutive sections incubated with normal

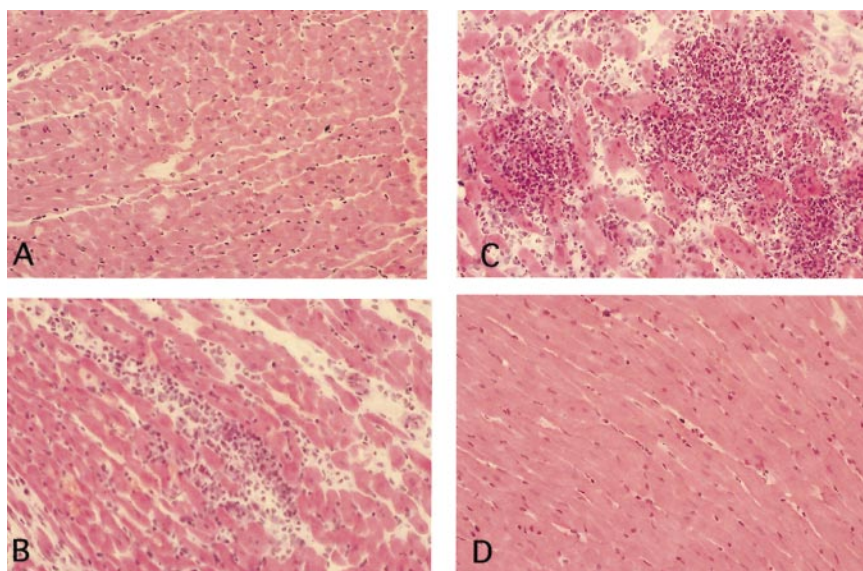


**FIGURE 1.** Pathologic grading of extent of inflammatory damage. Mild damage (A), moderate damage (B), severe damage (C), and normal control (D). ( $\times 200$ ).

rabbit IgG were used as negative controls, and sections from normal nonfasted rats were used as positive controls.

GLUT expression was visually evaluated and divided on the basis of microscopic findings into the following four grades: 0, no expression; 1, minimal expression; 2, expression between those of 1 and 3; and 3, the strongest expression seen in any of the specimens.

### Statistical Analysis

Data are expressed as the mean  $\pm$  SD. Groups were compared by ANOVA with a multiple comparison test. A value of  $P < 0.05$  was considered to indicate a statistically significant difference.

## RESULTS

### Body Weight and Heart Weight

In both the acute and subacute phase (each  $n = 5$ ) of myocarditis, body weight was significantly lower than in the control rats ( $225.9 \pm 15.8$  g [acute] vs.  $322.8 \pm 17.7$  g;  $309.8 \pm 26.7$  g [subacute] vs.  $386.8 \pm 31.2$  g;  $P < 0.0001$ ). In the chronic phase, however, body weight was not significantly different from that of the controls ( $395.1 \pm 40.1$  g vs.  $413.6 \pm 32.0$  g; not significant [NS]). In both the acute and the chronic phase, heart weight was significantly greater than in the controls ( $2.0 \pm 0.5$  g [acute] vs.  $1.0 \pm 0.1$  g;  $P < 0.0001$ ;  $1.8 \pm 0.6$  g [chronic] vs.  $1.1 \pm 0.1$  g;  $P < 0.0001$ ).

### Total Cardiac Uptakes of DG and $^{201}\text{Tl}$

The total cardiac uptake of DG in the acute phase of myocarditis ( $n = 5$ ) was significantly increased in comparison with the control uptake ( $n = 5$ ) ( $3.43\% \pm 0.92\%$  vs.  $0.97\% \pm 0.38\%$ ;  $P < 0.0001$ ). In the subacute phase, the total DG uptake was significantly decreased in comparison with the acute phase ( $1.97\% \pm 0.53\%$  vs.  $3.43\% \pm 0.92\%$ ;  $P < 0.001$ ). A decrease was seen in the chronic phase ( $n = 5$ ), but the total DG uptake was still higher than in the controls ( $1.85\% \pm 0.37\%$  vs.  $0.97\% \pm 0.38\%$ ;  $P < 0.01$ ). The total  $^{201}\text{Tl}$  uptake in myocarditis was significantly reduced in comparison with that of the controls in the acute phase ( $7.4\% \pm 0.7\%$  vs.  $12.0\% \pm 3.3\%$ ;  $P < 0.005$ ), but it recovered to the control uptake in the chronic phase ( $13.0\% \pm 3.3\%$  vs.  $12.0\% \pm 3.3\%$ ; NS) (Fig. 2).

### Regional Uptakes of DG and $^{201}\text{Tl}$

Acute-phase autoradiograms of DG and  $^{201}\text{Tl}$  are shown in Figures 3A and B, and chronic-phase autoradiograms are shown in Figures 3C and D.

In the acute phase, the myocardial distribution of DG was different from that of  $^{201}\text{Tl}$ . The regional myocardial uptake in each ROI was normalized by that of the corresponding control. DG uptake was increased significantly in the area of severe inflammation in comparison with the controls ( $317.5\% \pm 103.3\%$  vs.  $100\% \pm 46.4\%$ ;  $P < 0.0005$ ), but it was not increased in the areas of moderate ( $169.6\% \pm 59.9\%$ ) and slight ( $143.1\% \pm 107.9\%$ ) inflammation. Most of the areas with high DG uptake were located within the inflammatory foci. A few areas of high DG uptake were located at normal myocardial areas. In these areas,  $^{201}\text{Tl}$  uptakes were within the normal limit without exception. In the subacute phase, no areas of severe inflammation were found. In the moderate inflammation areas, DG uptake was significantly increased in comparison with the controls ( $367.1\% \pm 175.4\%$  vs.  $100\% \pm 12.8\%$ ;  $P < 0.0005$ ). In the chronic phase, there were no severe inflammatory foci, but some areas of high DG uptake were observed in the pericardium. Regional DG uptake in the moderate infiltration areas was similar to that of the controls ( $129\% \pm 43\%$  vs.  $100\% \pm 48\%$ ; NS) (Table 1).

$^{201}\text{Tl}$  uptake in the acute phase gradually decreased in parallel to the subsiding of inflammation and recovered to the control level in areas of mild infiltration ( $88.4\% \pm 31.9\%$  vs.  $100.0\% \pm 11.4\%$ ; NS). In the subacute phase, the regional  $^{201}\text{Tl}$  uptake was restored to the normal level in areas of moderate and mild infiltration ( $83.7\% \pm 23.1\%$  [moderate] vs.  $100.0\% \pm 23.0\%$ ; NS;  $109.5\% \pm 27.2\%$  [mild] vs.  $100.0\% \pm 23.0\%$ ; NS). In the chronic phase, the regional  $^{201}\text{Tl}$  uptake in the moderate and mild infiltration areas did not differ from that of the controls ( $76.6\% \pm 29.6\%$  [moderate] vs.  $100.0\% \pm 7.5\%$ ; NS;  $100.2\% \pm 25.4\%$  [mild] vs.  $100.0\% \pm 7.5\%$ ; NS) (Table 1).

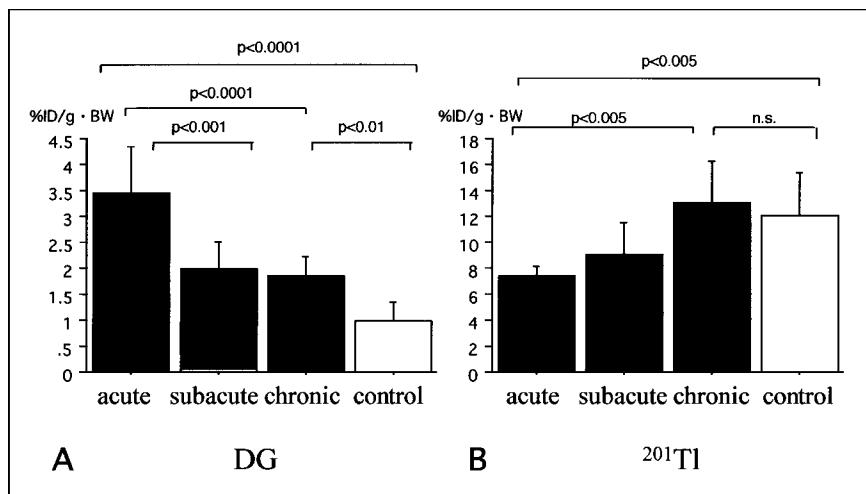
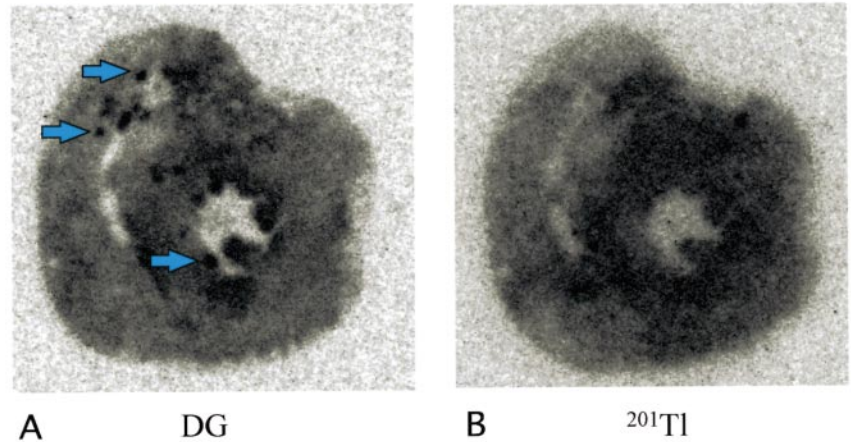


**FIGURE 2.** Total cardiac uptakes of DG (A) and  $^{201}\text{Tl}$  (B) in acute, subacute, and chronic phases of myocarditis. Open and closed bars indicate average values of all phases in controls and myocarditis, respectively.

## Acute Phase



## Chronic Phase

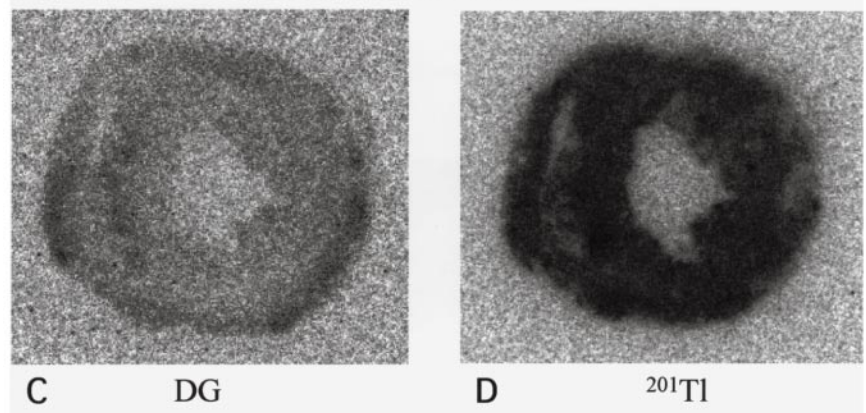


**FIGURE 3.** Dual-tracer autoradiograms of myocardium in acute (A and B) and chronic (C and D) phases of autoimmune myocarditis. Arrowheads denote sites of severe infiltration corresponding to areas of high GLUT1 expression. DG image (A and C) and  $^{201}\text{Tl}$  image (B and D).

### Expressions of GLUT1 and GLUT4

In the acute phase of myocarditis, scattered inflammatory foci of various sizes were observed in the myocardium and some overlapped sites of GLUT1 expression (Figs. 4A and B). Moreover, some of the GLUT1 expression sites also corresponded to areas of high DG uptake (Fig. 3A). Areas of myocardium with few infiltrating cells, on the other hand, corresponded to GLUT4 expression sites (Fig. 4C).

In the chronic phase, all foci of infiltration were replaced by fibrosis. No foci of severe inflammation were observed, and GLUT1 and GLUT4 were expressed homogeneously throughout the section except in areas with scarring (Figs. 4D–F).

Regional analysis showed grade 3 GLUT1 expression, especially in the areas of severe infiltration in the acute phase ( $2.87 \pm 0.30$  vs.  $0.87 \pm 0.30$ ;  $P < 0.0001$ ). In the chronic phase, typical GLUT1 findings were absent (Table 2).

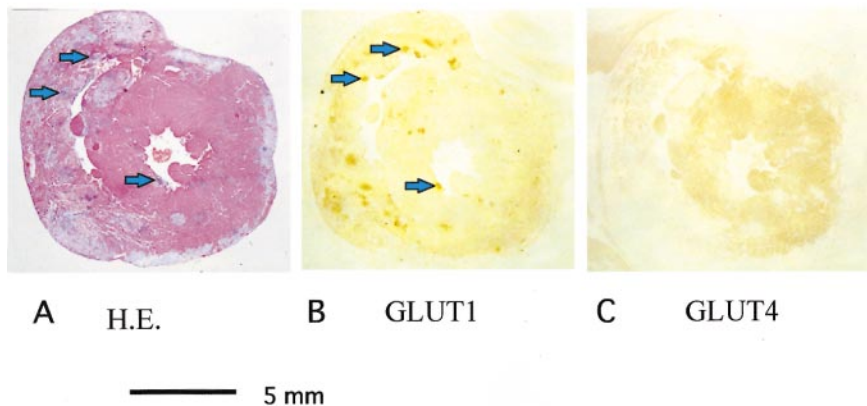
**TABLE 1**  
Regional Uptakes of DG and  $^{201}\text{Tl}$

Phase	DG (%)				$^{201}\text{Tl}$ (%)			
	Severe	Moderate	Mild	Control	Severe	Moderate	Mild	Control
Acute	$317.5 \pm 103.3^*$	$169.6 \pm 59.9$	$143.1 \pm 107.9$	$100.0 \pm 46.4$	$48.4 \pm 21.5^\dagger$	$72.1 \pm 34.6$	$88.4 \pm 31.9$	$100.0 \pm 11.4$
Subacute	—	$367.1 \pm 175.4^*$	$245.7 \pm 61.0$	$100.0 \pm 12.8$	—	$83.7 \pm 23.1$	$109.5 \pm 27.2$	$100.0 \pm 23.0$
Chronic	—	$129.0 \pm 43.3$	$124.9 \pm 59.8$	$100.0 \pm 48.2$	—	$76.6 \pm 29.6$	$100.2 \pm 25.4$	$100.0 \pm 7.5$

\*  $P < 0.0005$  vs. control.

†  $P < 0.005$  vs. control.

### Acute Phase



### Chronic Phase

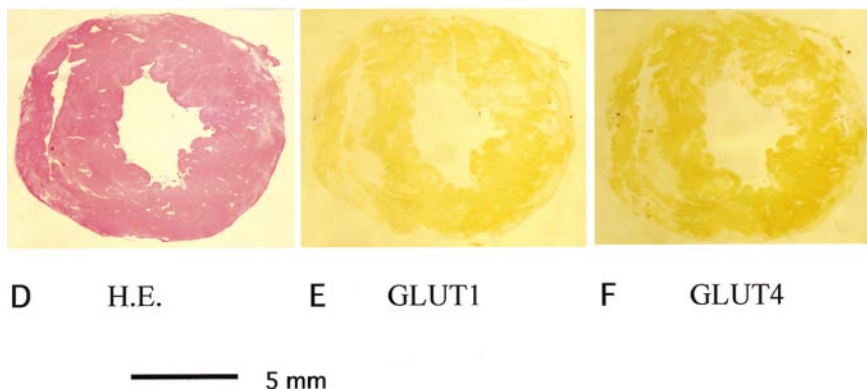


**FIGURE 4.** Microscopic findings in acute (A–C) and chronic (D–F) phases of myocarditis. Hematoxylin and eosin (H.E.) staining (A and D), GLUT1 (B and E), and GLUT4 (C and F). Arrowheads indicate sites of high DG uptake ( $\times 1$ ).

Grade 2 expression of GLUT4 was observed in the areas of mild infiltration in the acute phase ( $1.87 \pm 0.30$  vs.  $1.07 \pm 0.15$ ;  $P < 0.0005$ ). In the chronic phase, typical GLUT4 findings were absent (Table 2).

### DISCUSSION

We investigated myocardial damage in myocarditis using ex vivo dual-tracer autoradiography with DG and  $^{201}\text{Tl}$ . The uptakes of DG and  $^{201}\text{Tl}$  varied with the severity of inflammation, and neither showed homogeneous uptake. These findings suggest that FDG PET and myocardial SPECT with  $^{201}\text{Tl}$  are potentially useful for assessing the severity of myocarditis.

In previous studies, the positive scintigraphic tracers  $^{99\text{m}}\text{Tc}$ -pyrophosphate (3),  $^{67}\text{Ga}$ -citrate (4,5),  $^{131}\text{I}$ -antimyosin monoclonal antibody (5), and  $^{111}\text{In}$ -antimyosin Fab (4,6) were shown to be capable of detecting myocarditis. Furthermore,  $^{99\text{m}}\text{Tc}$ -pyrophosphate can detect myocardial necrosis. However, the inability of  $^{99\text{m}}\text{Tc}$ -pyrophosphate to detect either the center of a necrotic focus or its margin is prob-

lematic.  $^{67}\text{Ga}$ -citrate can detect inflammation but with unsatisfactory sensitivity.  $^{111}\text{In}$ -antimyosin Fab was found to be capable of detecting myocarditis in a previous experiment and a clinical study. Yasuda et al. (6) reported the sensitivity of  $^{111}\text{In}$ -antimyosin Fab in detecting myocarditis to be 61%. The problem with  $^{111}\text{In}$ -antimyosin Fab is that image acquisition is a 48-h process. There have been no clinical reports on the detection of myocarditis in the acute phase by FDG PET. However, inflammatory cells in tissue can be detected by FDG (7,8), and FDG PET is reportedly more useful than  $^{67}\text{Ga}$ -citrate in making a diagnosis of sarcoidosis (8). Consequently, FDG PET is considered to be better than the other methods for detecting early inflammatory change.

The total cardiac DG uptake was significantly higher in rats with myocarditis than in control rats, and the histologic findings showed DG uptake to be much higher in areas of severe inflammation than in areas of slight inflammation. The expression of GLUT1 was significantly increased in areas of severe infiltration in the acute

**TABLE 2**  
Visual Evaluation of Regional GLUT1 and GLUT4 Expressions

Phase	GLUT1 (degree)				GLUT4 (degree)			
	Severe	Moderate	Mild	Control	Severe	Moderate	Mild	Control
Acute	2.87 ± 0.30*	1.73 ± 0.68	0.93 ± 0.15	0.87 ± 0.30	0.20 ± 0.30	1.60 ± 0.44	1.87 ± 0.30†	1.07 ± 0.15
Subacute	—	1.73 ± 0.68	0.87 ± 0.30	0.93 ± 0.15	—	1.20 ± 0.30	1.93 ± 0.15	1.40 ± 0.55
Chronic	—	1.00 ± 0.62	0.87 ± 0.51	0.93 ± 0.15	—	1.07 ± 0.76	1.40 ± 0.28	1.40 ± 0.55

\*  $P < 0.0001$  vs. control.

†  $P < 0.0005$  vs. control.

phase. Severe infiltration was observed in hearts affected by myocarditis; infiltrating cells were thus considered to be primarily responsible for the increase in DG uptake. In contrast,  $^{201}\text{Tl}$  uptake was significantly lower than in normal controls.

In cardiac specimens from rats with acute-phase myocarditis, which were stained with hematoxylin and eosin, areas of severe cell infiltration merged and produced foci. GLUT1 was mainly expressed in inflammatory foci, whereas GLUT4 was expressed in the myocardium with minimal cellular infiltration. The locations of inflammatory foci corresponded to areas showing GLUT1 expression and high DG uptake. This observation was considered to indicate that the infiltrating cells increased DG uptake through enhanced GLUT1 expression. Total cardiac uptake of DG also depended on the number of infiltrating cells. In contrast, little  $^{201}\text{Tl}$  uptake occurred in the inflammatory foci. The  $^{201}\text{Tl}$  kinetics depend on the Na/K pump in the cell membrane (10), suggesting that none of the myocardial cells within the foci had functioning Na/K pumps in their cell membranes. Thus, the finding of low  $^{201}\text{Tl}$  uptake can be considered an indication of myocardial cell damage.

In the acute phase of myocarditis, DG uptake definitely depended on the extent of cell infiltration, whereas in the subacute and chronic phases, it was increased in comparison with the controls despite the small number of infiltrating cells. Heart failure increases the levels of plasma catecholamines and insulin, and these hormonal factors have been suggested to alter myocardial metabolism (11,12).  $^{201}\text{Tl}$  uptake is thought to have been restored to the control level because Na/K pump function in the myocardium recovered.

In the clinical setting, FDG PET and  $^{201}\text{Tl}$  SPECT are excellent methods for detecting myocardial ischemia, myocardial viability, and myocardial damage. Although FDG uptake does not usually occur in normal myocardium during fasting, ischemia induces translocation of GLUT1 and GLUT4 in the myocardium (12), and FDG uptake consequently increases in ischemic myocardium. In our experiment, however, infiltrating cells showed an apparent increase in cardiac DG uptake during myocarditis. No relationship was seen between ischemia

caused by coronary stenosis and this increased DG uptake. Clinically, high FDG uptake does not always reflect ischemia in the myocardium, but it is possible that infiltrating cells are responsible for the increased FDG uptake in the setting of myocarditis. Heterogeneous distribution of FDG sometimes is seen for unknown reasons in the healthy subject after fasting (13). It is difficult to discriminate between normal myocardium and infiltration cells in myocarditis in subacute and chronic phases. In the acute phase in this study, however, the area with high FDG uptake and low  $^{201}\text{Tl}$  uptake occurred at the area of infiltrating cells. The detection of infiltration foci in myocarditis in the acute phase is a significant finding.

## CONCLUSION

The results of our study show increased cardiac DG uptake in the acute phase of autoimmune myocarditis, whereas  $^{201}\text{Tl}$  uptake is decreased. The increased DG uptake in the acute phase was caused by increased GLUT1 expression in the infiltrating cells. Therefore, FDG can be used as a positive tracer to detect myocarditis, and  $^{201}\text{Tl}$  can be used as a negative tracer. The combination of FDG and  $^{201}\text{Tl}$  can show clearly whether or not severe infiltration is present in acute myocarditis.

## REFERENCES

1. Kawai C, Matsumori A, Fujiwara H. Myocarditis and dilated cardiomyopathy. *Ann Rev Med.* 1987;38:221–239.
2. Kodama M, Matsumoto Y, Fujiwara M, et al. A novel experimental model of giant cell myocarditis induced in rats by immunization with cardiac myosin fraction. *Clin Immunol Immunopathol.* 1990;57:250–262.
3. Matsumori A, Kadota K, Kawai C. Technetium-99m pyrophosphate uptake in experimental viral perimyocarditis. *Circulation.* 1980;61:802–807.
4. Morguet AJ, Munz DL, Kreuzer H, et al. Scintigraphic detection of inflammatory heart disease. *Eur J Nucl Med.* 1994;21:666–674.
5. Matsumori A, Ohkusa T, Matoba Y, et al. Myocardial uptake of antimyosin monoclonal antibody in a murine model of viral myocarditis. *Circulation.* 1989;79:400–405.
6. Yasuda T, Palacios IF, Dec GW, et al. Indium 111-monoclonal antimyosin antibody imaging in the diagnosis of acute myocarditis. *Circulation.* 1987;76:306–311.
7. Kubota R, Yamada S, Kubota K, et al. Intratumoral distribution of fluorine-18-fluorodeoxyglucose in vivo: high accumulation in macrophages and granulation tissues studied by microautoradiography. *J Nucl Med.* 1992;33:1972–1980.

8. Brudin LH, Valind S, Rhodes CG, et al. Fluorine-18 deoxyglucose uptake in sarcoidosis measured with positron emission tomography. *Eur J Nucl Med.* 1994;21:297–305.
9. Kodama M, Hanawa H, Saeki M, et al. Rat dilated cardiomyopathy after auto-immune giant cell myocarditis. *Circ Res.* 1994;75:278–284.
10. McCall D, Zimmer LJ, Katz AM. Kinetics of thallium exchange in cultured rat myocardial cells. *Circ Res.* 1985;56:370–376.
11. Raymond R, Renfu Y, Michael JC, et al. Additive effects of hyperinsulinemia and ischemia on myocardial GLUT1 and GLUT4 translocation in vivo. *Circulation.* 1998;98:2180–2186.
12. Young LH, Renfu Y, Russell R, et al. Low-flow ischemia leads to translocation of canine heart GLUT-4 and GLUT-1 glucose transporters to the sarcolemma in vivo. *Circulation.* 1997;95:415–422.
13. Marshall RC, Tillisch JH, Phelps ME, et al. Identification and differentiation of resting myocardial ischemia and infarction in man with positron computed tomography, <sup>18</sup>F-labeled fluorodeoxyglucose and N-13 ammonia. *Circulation.* 1983;67:766–778.